DETERMINATION OF DEFORMABILITY CHARACTERISTICS OF AZ31 MAGNESIUM ALLOY SHEETS

Gheorghe Brabie[1], Andrei Dragos Bors[2]

[1, 2] Vasile Alecsandri University of Bacau, Departament of Industrial Engineering
Calea Marasesti 157, Bacau, 600115, Romania

Corresponding author: Andrei Dragos Bors, andreidragosb@yahoo.com

Abstract: The experiments were done on AZ31 magnesium alloy sheets. The experiments were done by Nakazima test specifications. Hasek type specimens were used and the tests were performed for five different sizes. At the Nakazima test, approximately five specimens were used for each geometry. In total 28 specimens were used to determine the deformability characteristics. For the first type of specimens the average values for minor strain were about 0.028% and major strain were about 0.057%. For the last type of specimens the average values for minor strain were about -0.0447% and major strain were about 0.1004%.
Key words: Nakazima Test, Strain-stress diagram, Hasek specimens, Aramis System, forming limit diagram.

1. INTRODUCTION

The main problems that are studied by scientists regarding the magnesium alloys sheets are thouse related to malleability. The real problem is that the processing methods of these alloys differ greatly from other alloys that are used in the industry, like steel and aluminum. The most important advantage that magnesium alloys have is the low density. The second and third most commonly used alloys in industry are aluminum and steel, [1].
The Nakazima test consists of deforming specimens by using a hemispherical punch and a circular blankholder (BHF), figure 1.

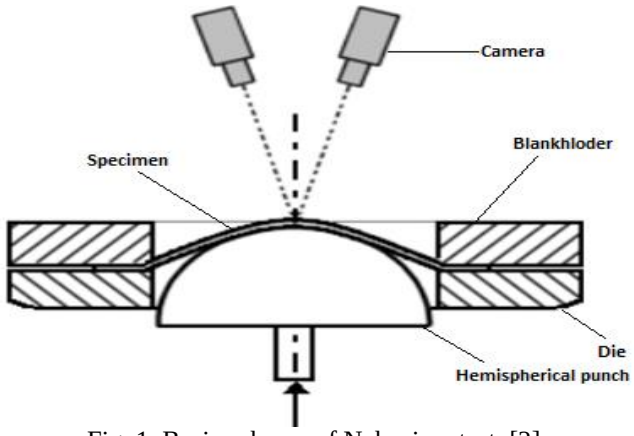

Fig. 1. Basic schema of Nakazima test, [2]

By modifying the width of the specimen and the lubrication conditions, deformation states are obtained between the uniaxial traction and the biaxial stretch, thus covering the entire deformation range of a forming limit curve. The paper tries to make a detailed assessment of the deformability properties of the AZ31 magnesium alloy in order to identify the conditions and the most efficient way in which this type of alloy can be used, taking into account the advantages and disadvantages that it can offer.

2. EXPERIMENTAL

The testing equipment is made from a hydraulic press and the Aramis video system (figure 2). Tests were performed on Hasek specimens of AZ31 magnesium alloy sheet.

Fig. 2. Testing installation for Nakazima test

The tested specimens are presented in fig.3 and their dimensions are shown in table 1.
In the experimental program, the measurement of the boundary deformations and the biaxial stress was obtained through the Aramis system. For strains measurements using the Aramis system, four steps have to be taken: preparation of specimens; acquisition of images; image processing; results analysis. In a first phase, the surface of the specimen is covered with a white paint and a gassing layer is then applied with a black paint spray to form the points to be traced during

the deformation test. Figure 4 shows some specimens prepared for the Nakazima test.

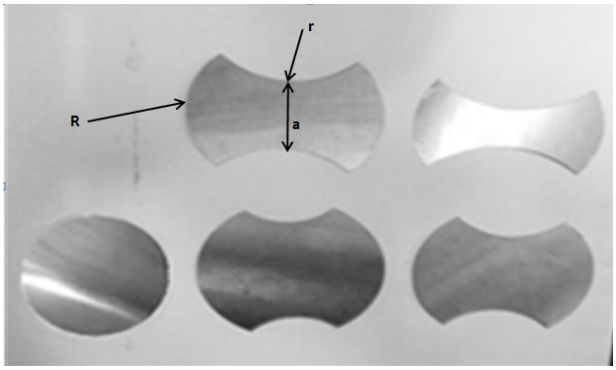

Fig. 3. Shapes of Hasek testing specimens (R- external circle radius, r- side circle radius and a- distance between side circles – width of the specimen)

Table 1. Hasek specimen dimensions

No.	Dimensions		
	R [mm]	r [mm]	a [mm]
1	100	110	50
2	100	95	90
3	100	80	110
4	100	65	140
5	100	0	200

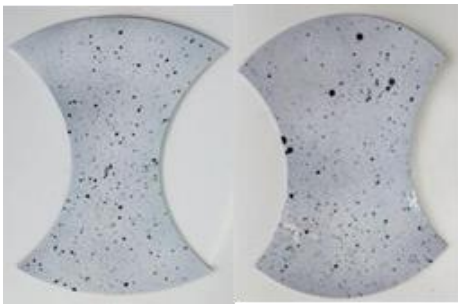

Fig. 4. Prepaired specimens for Nakazima test

Once the specimen has been painted, it is possible to pass to the next phase, image acquisition during the deformation process. These images will be used to calculate deformations. To analize the forming limit parameters images are recorded until a crack occurs. (figure 5).

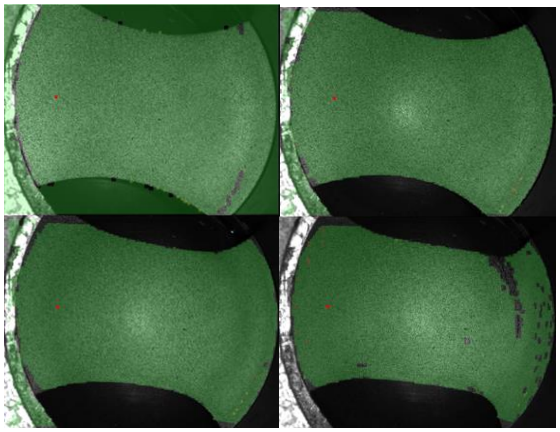

Fig. 5. Recorded images in different stages of deformation process.

During the image processing stage, the Aramis program automatically analyzes the displacements of points on the surface of the specimen using the photogrammetry principle. At the end of this analysis, a deformation distribution map is displayed, figure 6.

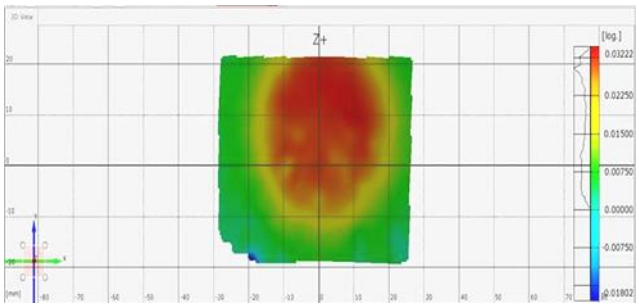

Fig. 6. Map of the main deformation distribution

During the tests, images of the specimens were captured using both the special test equipment and the camera. The images captured by the cameras of the testing equipment are used exclusively for the determination of strains occurred during the tests. Images captured with the camera are used only to show and compare the different stages through which the test specimen passes during the test. Figure 7a and 7b shows the moment when cracks occur on the surface of the specimen during the test.

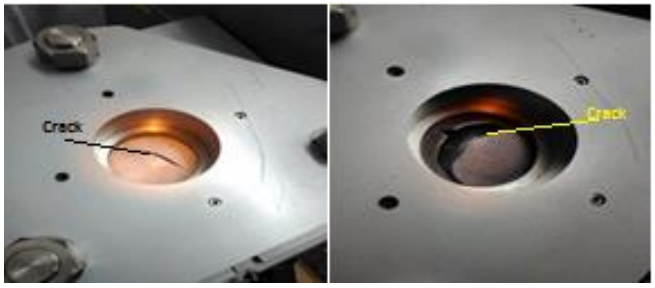

Fig. 7. Moment of crack occured during the Nakazima test

Upon completion of the tests, the specimens were photographed to show the deformation mode and cracks. Figure 8 shows the images of the deformed specimens.

Fig. 8. Deformation of the test specimens after the Nakazima test

When the punch touches the specimen and acts on its surface, it begins to deform the specimen effectively. As the punch acts stronger, the deformation is stronger

and propagates from the middle to the edges of the specimen (figure 6). The moment when the specimen deformation reaches maximum values is that before cracks or tears occur. When the first crack occurs, the deformation of the specimen is maximum and the flow limit of the material has been reached. The maximum deformation of the material means that it is stretched and thinned at the same time until at the molecular level had instability of the granular structure.
In figure 9 are both real-time captured images of testing cameras and graphical analysis performed by the Aramis system.

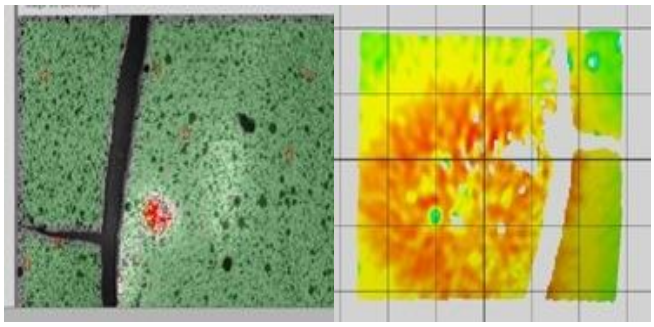

Fig. 9. Moment when crack occur

As it can be seen in the above figure, the stresses and deformations have reached maximum values in the crack area. Figure 9 shows the moment when the specimen broke from punch pressure on the analyzed area, which is also the end of the test.
After the crack initiating when the deformation of the specimen is maximal if the deformation process is continued, the crack propagates in different directions depending on the occurrence of the grain instability phenomenon in the molecular structure of the material specimen and ultimately the effective breakage of the specimen occour.
We can observe that the entire surface of the specimen shows a state of high tension and deformation which at the end of the specimen has broken.
Generally, the material yields in such situations in the areas where the specimen is narrower because in those areas both stresses and deformations grow faster. These areas are mainly tracked during the experimental tests. The material may also crack or brake due to manufacturing defects, imperfections resulting from the cutting or processing of the specimen.
With the help of the image analysis program in the ARAMIS system, the direction of displacement of the black dots on the surface of the specimen was tracked as the punch begins to act on the specimen and effectively begins the deformation process. In figure 10 there is shown an image in which the program indicates the direction of movement of each black dot on the surface of the specimen that it has been able to track from the start of the test to the end of the test. Practically, the video camera program tracks the black paint dots that were applied in the preparation stage of the specimen.

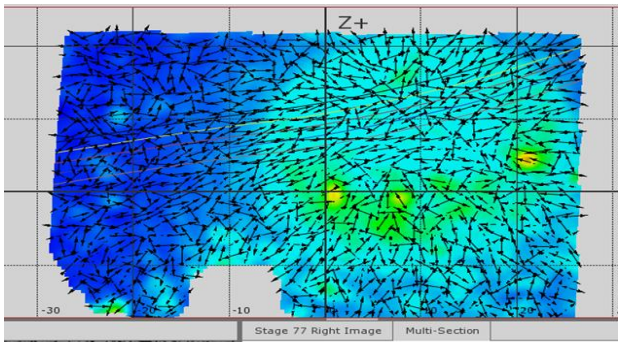

Fig. 10. Analysis of the displacement of black dots on the surface of the specimen during the test

It should be noted that some black dots on the surface of the specimen can not be tracked by the program until the end of the test because the material in its deformation process can deform exactly from the area where the point is applied and thus it changes its geometry and dimensions and then it can't be recognized after its original parameters. Another reason why the program can not track all the black dots from the beginning of the test and until the end of the test is that some black dots due to the deformations may come out of the visual field of the cameras. The measurements made by the program are based on the movement of the black dots in order to increase or decrease the distances between them.
Using the image analysis program in the ARAMIS system, the direction of displacement of the black dots on the surface of the specimen was monitored when the deformation of the specimen was maximal and, implicitly, the test was completed. Figure 11 shows this in plane 2D.

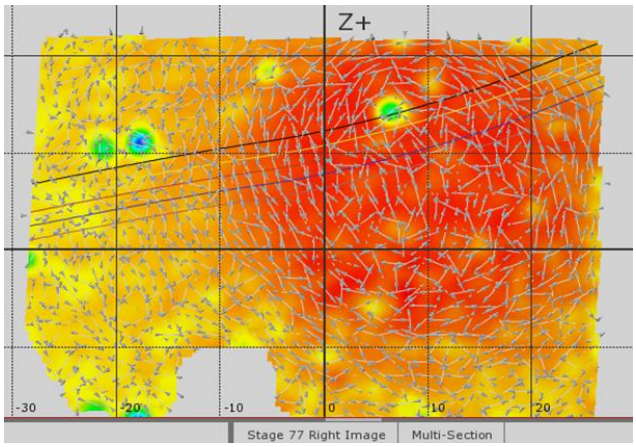

Fig. 11. Analysis of the displacement of black dots on the surface of the specimen at the end of the test

In figure 11 it can be seen how in the area where the punch is acting, the deformation of the specimen material is approximately circular in plane 2D and spherical in 3D plane. The direction of the arrows following the displacement of the points on the surface of the blank is approximately circular in the area where the deformation is higher as a result of the

action of the punch, and as we go further towards the edges of the specimen, the longitudinal deformations begin to appear, which means that the specimen stretches from the areas where the press retaining ring acts and narrows from the remaining free zones, appearing in those areas the phenomenon of necking.

3. RESULTS AND DISCUSSIONS

To select the optimal values of major strain and minor strain, it can be applied a section in the area where the crack or rupture occurred and select the values recorded before the crack appeareance, because in that section was recorded the maximum deformation point of the specimen material before that instability occurred of the molecular structure of the material mentioned above.

Figure 12 shows a printscreen in which we can see how data is being analyzed. On to the bottom left side, it can be seen the real time picture of the video camera specimen.

At the top of the print-screen it can be seen the image of the specimen processed by the image analysis program, in which we can observe the selected section for extracting the data to construct the forming limit diagram.

On the bottom right side of the printscreen, we obtain the graph with the values recorded in the selected section from the start of the test until the test is complete.

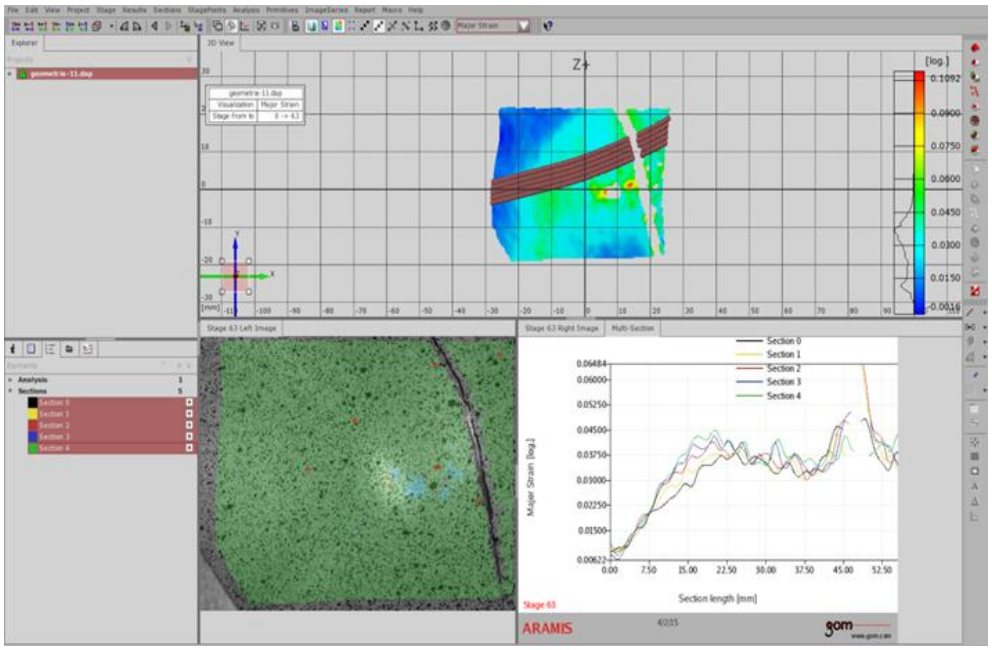

Fig. 12. Drawing the section of the specimen; chart of values for the section

The next step in constructing the forming limit diagram is to collect the datas (table 2) with all the values recorded for each of the five geometries and for each of the five tests performed for each geometry separately.

Table 2. Values of minor and major strains

Geometry	Minor strain (%)	Major strain (%)
0-1	0.0300	0.0600
0-2	0.0320	0.0510
0-3	0.0220	0.0600
0-4	0.0315	0.0581
0-5	0.0311	0.0555
1-1	0.0120	0.0450
1-2	0.0180	0.0445
1-3	0.0200	0.0440
1-4	0.0175	0.0444
1-5	0.0130	0.0450
2-1	0.0230	0.0730
2-2	0.0140	0.0680
2-3	0.0230	0.0730
2-4	0.0100	0.0650
2-5	0.0155	0.0685
3-1	-0.0140	0.0750
3-2	-0.0180	0.0730
3-3	-0.0290	0.0685
3-4	-0.0500	0.0650
3-5	-0.0315	0.0689
4-1	-0.0520	0.1300
4-2	-0.0450	0.1100
4-3	-0.0490	0.1060
4-4	-0.0325	0.0710
4-5	-0.0450	0.0850

In tables 3 and 4 there are presented the average values of minor and major strains that will be used to construct the forming limit diagram (FLD).

Table 3. Average values of minor and major strains

Geometry	Average minor strain (%)	Average major strain (%)
0	0.0280	0.0570
1	0.0160	0.0445
2	0.0165	0.0690
3	-0.0320	0.0700
4	-0.0447	0.1004

Table 4. Values of minor and major strains used to build forming limit diagram (FLD)

Geometry	Minor strain (%)	Major strain (%)
5	-0.0447	0.1004
4	-0.0320	0.0700
3	0.0019	0.0425
2	0.0160	0.0445
1	0.0280	0.0570

The purpose of all the steps taken up to now is the realization of the forming limit diagram, figure 13. This chart is designed to characterize the quality of the material and defines two areas: the rupture area and the necking area, [3, 4]. The curves shown on the chart represent the critical points in which cracks are expected to occur. Between the two areas (safe area and breakage area), separated by the FLD, there is also a critical deformation zone, [5].

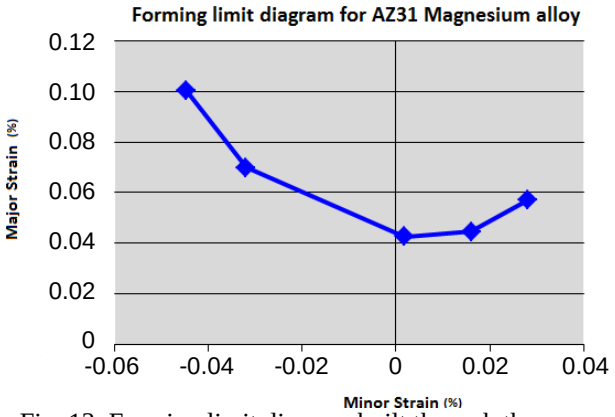

Fig. 13. Forming limit diagram built through the average values of the minor and major strains

4. CONCLUSIONS

The formability characteristics of magnesium sheets are determined by carrying out the Nakazima test. The tests tracked the behavior of the material on different specimen dimensions. The tables show the values of minor and major strains. These values were determined using the Aramis system.

In order to compare the results obtained from the performed experiments, similar data were also considered for different alloys such as steel and aluminum. Minor strain value for steel alloy is 0.51% at the maximum point opposed to 0.11% for magnesium alloy. Also, the major strain value for steel alloy comes into the negative area up to -0.31% and only -0.05% for magnesium alloy. If we look at the values of the major strain in the positive area, we will notice that the differences are still big, meaning for steel alloy obtained values of 0.38% and for the magnesium alloy were obtained values of 0.058%. Minor strain values for the steel alloy are 0.51% at the maximum point as opposed to 0.11% for the magnesium alloy, [6].

Magnesium sheets are very often used in both the automotive and aerospace industries for the production of parts. The main advantage that these parts offer is that of low specific weight, [7].

5. REFERENCES

1. Luo A. A. (2006), *Wrought magnesium alloys and manufacturing processes for automotive applications*, Lightweight Magnesium Technology, 155-165.
2. Available from: http://www.gom.com/fileadmin/user_upload/industries/flc_fld_EN.pdf, Accesed: 13/01/2016
3. Butuc M.C., Barata da Rocha A., Gracio J. J. and Ferreira Duarte J., (2002), *A more general model for forming limit diagrams prediction*, Journal of Materials Processing Technology, 125–126(9), 213–218.
4. Jurco P., Banabic D., (2005), *A user-frienldy programme for calculating Forming Limit Diagrams*, In: Banabic D (ed) Proc. of the 8th ESAFORM Conference on Material Forming, Cluj Napoca, pp. 423-427.
5. Available from: http://www.gom.com/industries/sheet-metal-forming/material-propertiesflc.html, Accesed: 13/01/2016
6. Slota J., Spisak E., (2005), *Comparison of the forming limit diagram (FLD) models for drawing quality (DQ) Steel sheets*, Metalurgija, 44(4), 249-253.
7. Mordike B.L., Ebert T., (2001), *Magnesium: Properties - applications –potential*, Mater. Sci. Eng. A302, 37-45.
8. Comaneci R., Nedelcu D., Bujoreanu L.G., (2017). *Influence of tools geometry and processing conditions on behavior of a difficult-to-work Al-Mg alloy during equal channel angular pressing*, AIP Conference Proceedings 1896, 200004 (2017); doi: 10.1063/1.5008241
9. Gina Mihaela Sicoe, Iacomi Doina, Iordache Monica, Nitu Eduard, *Numerical modelling of the process of cold plastic deformation with planetary rollers*, International Journal of Modern Manufacturing Technologies, V(1), 105-112.

Received: April 20, 2017 / Accepted: December 10, 2017 / Paper available online: December 20, 2017 © International Journal of Modern Manufacturing Technologies.